EG&G
ENERGY MEASUREMENTS

EGG-10282-1103
UC-41
JANUARY 1988

THE
**REMOTE SENSING LABORATORY**
OPERATED FOR THE U.S.
DEPARTMENT OF ENERGY BY EG&G/EM

AN AERIAL RADIOLOGICAL SURVEY OF THE

# KENNEDY SPACE CENTER AND CAPE CANAVERAL AIR FORCE STATION

TITUSVILLE, FLORIDA

DATE OF SURVEY: OCTOBER 1985

## DISCLAIMER



Printed in the United States of America.

Available from:

National Technical Information Service
U.S. Department of Commerce
5285 Port Royal Road
Springfield, Virginia 22161

NTIS price codes

Printed copy: A02
Microfiche copy: A01

EGG--10282-1103

DE89 001862

EG&G
ENERGY MEASUREMENTS

AN AERIAL RADIOLOGICAL SURVEY OF THE

# KENNEDY SPACE CENTER AND CAPE CANAVERAL AIR FORCE STATION

AND SURROUNDING AREA

TITUSVILLE, FLORIDA

DATE OF SURVEY: OCTOBER 1985

H. W. Clark
Project Scientist

REVIEWED BY

W. J. Tipton, Assistant Manager
Aerial Measurements Operations

This Document is UNCLASSIFIED

C. K. Mitchell
Classification Officer

This work was performed by EG&G/EM for the United States Department of Energy, Office of Nuclear Safety, under Contract Number DE-AC08-83NV10282

## ABSTRACT

An aerial radiological survey of the entire Kennedy Space Center (KSC) and Cape Canaveral Air Force Station (CCAFS) was performed during the period 9 through 23 October 1985. This survey was conducted in three parts. First, a low resolution, low sensitivity background survey was performed that encompassed the entire KSC and CCAFS area. Next, two smaller, high resolution, high sensitivity surveys were conducted: the first focused on Launch Complexes 39A and 39B, and the second on the Shuttle Landing Facility. The areas encompassed by the surveys were 200, 5.5, and 8.5 square miles (500, 14, and 22 sq km), respectively. The purpose of these surveys was to provide information useful for an emergency response to a radiological accident. Results of the background survey are presented as isoradiation contour maps of both total exposure rate and man-made gross count superimposed on a mosaic of recent aerial photographs. Results of the two small, detailed surveys are also presented as an isoradiation contour map of exposure rate on the aerial photograph base. These data were evaluated to establish sensitivity limits for mapping the presence of plutonium-238. Natural background exposure rates at the Kennedy Space Center and Cape Canaveral Air Force Station are very low, generally ranging from 4 to 6.5 microroentgens per hour ($\mu$R/h) and less than 4 $\mu$R/h in wet areas. However, exposure rates in developed areas were observed to be higher due to the importation of construction materials not characteristic of the area.

# CONTENTS

## Tables



## Appendices

## 1.0 INTRODUCTION

An aerial radiological survey of the Kennedy Space Center (KSC) and Cape Canaveral Air Force Station (CCAFS), located near Titusville, Florida, was conducted during the period 9 through 23 October 1985. This survey was performed in support of the National Aeronautics and Space Administration (NASA) by the United States Department of Energy (DOE) utilizing the Aerial Measuring System which is operated for DOE by EG&G Energy Measurements, Inc. (EG&G/EM), Las Vegas, Nevada.[1] This work was conducted in preparation for two Space Shuttle launches, STS-61F and STS-61G. Each Shuttle will carry a spacecraft, Ulysses and Galileo, respectively, bound for Jupiter. All electrical power on board these spacecraft is provided by General Purpose Heat Source Radioisotope Thermoelectric Generators (GPHS RTGs) which are designed and built by DOE.[2] Two GPHS RTGs are used on board Galileo, while only one GPHS RTG is used on Ulysses. Electrical power is directly generated from the heat of decay of 132 kilocuries of plutonium-238 ($^{238}$Pu) in each RTG. In addition to the RTGs, Galileo carries 105 Light Weight Radioisotope Heater Units (LWRHUs), each containing 30 curies of $^{238}$Pu, for temperature stabilization of sensitive equipment.

The purpose of this survey was to provide information useful for an emergency response to a potential radiological accident relative to these or other future launches involving large quantities of radioactive material. The data provided by this survey document the present magnitude and spatial distribution of exposure rate and certain gamma-emitting nuclides, both natural and man-made. The survey data were also evaluated to determine the sensitivity limits for mapping the presence of $^{238}$Pu. It is also possible to detect $^{238}$Pu by measuring neutron and infrared emissions; however, these methods are not discussed here.

Should a radiological accident occur involving the RTGs, the survey would be repeated to map the spatial distribution of $^{238}$Pu and estimate the quantity present. After completion of cleanup operations, the area could again be surveyed and compared to previous surveys to measure the quality of the cleanup and assess the incident's net environmental impact. Unfortunately, the sensitivity of the aerial system was found to be less than desired because $^{238}$Pu emits very few gamma photons although it does emit an enormous number of alpha particles. Therefore, ground-based measurements would be required in areas where the degree of contamination is less than that detectable by the aerial system but still possibly of significance.

The survey was conducted in three parts: a low resolution, low sensitivity background survey, which encompassed the entire KSC and CCAFS area, and two smaller, high resolution, high sensitivity surveys which focused on the most probable areas to be affected if an accident should occur. These areas are the Space Shuttle launch sites (Launch Complexes 39A and 39B) and the Shuttle Landing Facility (SLF). The two detailed surveys were conducted as if searching for and mapping the presence of $^{238}$Pu.

Aerial radiological detection systems are capable of not only detecting regions of enhanced radiation, but also determining the area-averaged surface exposure rate and the specific nuclide(s) responsible for any anomaly. However, since these systems average exposure rates due to gamma-emitting radionuclides over a large area (several hectares), aerial measurements may significantly underestimate the intensity of localized sources of enhanced radiation as compared to ground-based measurements. The effect becomes increasingly more pronounced as the spatial extent of a source of radiation is made small with respect to the large area averaged by the airborne detection system. Therefore, ground surveys may also be necessary to accurately define the extent and intensity of highly localized anomalous areas.

Aerial detection systems are also sensitive to airborne sources of radiation (e.g., atmospheric radon gas and daughters or natural sources aboard the aircraft) in addition to cosmic rays. An estimate of the airborne source contribution has been extracted from the reported results. A cosmic ray exposure rate contribution of 3.7 microroentgens per hour ($\mu$R/h) has been added. Hence, the present results represent total external exposure rate due to terrestrial sources and cosmic rays only.

It is customary to report survey results as radiation exposure rates in $\mu$R/h extrapolated to 1 meter above ground level. The maximum annual radiation exposure, 24 hours per day for 365 days, due to external irradiation is related only to duration of exposure, so the total dose can be expressed in millirem per year (mrem/y) by multiplying the reported exposure rate in μR/h by 8.76. However, this dose rate relates only to external sources of radiation and does not reflect contributions due to inhalation, ingestion, or any other internal source (body burden) of radioactive material. Therefore, the actual amount of radiation absorbed by tissue depends on the circumstances as well as the duration of exposure.

## 2.0 NATURAL BACKGROUND RADIATION

Background radiation originates from naturally-occurring radioactive elements present in the earth (terrestrial radiation) and cosmic rays entering the earth's atmosphere from space. The terrestrial gamma rays originate primarily from the uranium decay chain, the thorium decay chain, and radioactive potassium. Variable concentrations of these nuclides produce estimated annual background radiation doses in the United States of about 15 to 140 mrem/y. The higher background radiation dose levels (up to 140 mrem/y) are found in western states, primarily in the Colorado Plateau area, and are a result of high uranium and thorium concentrations in surface minerals.

The thorium and uranium decay chains include radon—a radioactive, chemically inert gas—that diffuses through the soil and into the atmosphere. The rate of diffusion is highly variable, and the atmospheric distribution of radon can be complex due to a variety of factors. Thus, the magnitude of the background radiation contributed by airborne radon and its daughters depends on the meteorological conditions and the mineral composition and permeability of the soil as well as other physical conditions existing at each location at any particular time. Typically, radon contributes from 1 to 10% of the natural external background radiation exposure.

Cosmic rays produce another source of natural background radiation. Exposure rates due to cosmic rays vary primarily with elevation and slightly with latitude. Estimated dose rates range from 26 mrem/y at sea level in south Florida to 200 mrem/y at the higher elevations in the Rocky Mountains.

Cosmic ray exposure rates reported for elevations and latitudes comparable to those at KSC vary from 3.4 to 3.9 μR/h.[3,4] A value of 3.7 μR/h (60 mrem/y) has been adopted for this report.

## 3.0 SURVEY SITES

The Kennedy Space Center and Cape Canaveral Air Force Station are the principal space vehicle launch sites for the United States. KSC is operated by the National Aeronautics and Space Administration. Launches from KSC are primarily civilian. CCAFS is operated by the U.S. Air Force Systems Command, Eastern Space and Missile Center. Facilities there are made available to all branches of the military and government. Launches from CCAFS are now generally military.

The Kennedy Space Center is located along the eastern Atlantic coastline just east of Titusville, Florida on Merritt Island. Although KSC is entirely located on Merritt Island, it does not occupy the whole island. The community of Merritt Island and many private lands, mostly orchards and residences, occupy the southern portion of the island. The Cape Canaveral Air Force Station is entirely located on the Cape Canaveral Peninsula just to the southeast of Merritt Island. CCAFS occupies almost the whole cape except for Port Canaveral and the town of Cape Canaveral. KSC lies within the boundary of the Merritt Island National Wildlife Refuge. Together, KSC and CCAFS occupy over 200 square miles (500 square kilometers). This area is largely comprised of marshes and wetlands; drier areas are generally heavily overgrown with brush and trees. Many technical support sites and industrial areas are scattered widely throughout this area. All launch sites are near the Atlantic shoreline. Complexes 39A and 39B are the northernmost launch pads in a long chain that extends along the shore to the south. The Shuttle Landing Facility is an enormous, 15,000-foot (4.6-kilometer) long runway that parallels Kennedy Parkway less than 5 miles (8 kilometers) northwest of the Vehicle Assembly Building (VAB).

## 4.0 SURVEY EQUIPMENT AND PROCEDURES

The survey of KSC and CCAFS was conducted in three segments. The equipment and procedures employed to perform these surveys are reviewed briefly in this section as well as the data analysis techniques. Detailed discussions of the equipment and procedures can be found in previously published reports.[5,6]

### 4.1 Aerial Measurements

The Aerial Measuring System, comprised of a radiation detector package and a specialized data acquisition and recorder system (REDAR IV*), was mounted on board a high-performance helicopter.** The detector package utilized for this survey consisted of an array of eight NaI(Tℓ) "log" style scintillation detectors, each 4-in. square by 16-in. long (10.2 cm by 40.6 cm). These detectors were distributed equally between each of two cargo pods that were mounted on the landing skids of the helicopter. A small 4-in. diameter by 4-in. thick (10.2 cm by 10.2 cm) NaI(Tℓ) detector was also installed in one pod to measure radiation in very high gamma flux areas. Signals from the eight log detectors were summed to produce a single spectrum with high sensitivity. The signal from the small detector was used to provide a spectrum with lower sensitivity for use in areas exhibiting greatly enhanced levels of radiation. Both spectra were simultaneously acquired and recorded. Hence, the count rate operating range of the data acquisition system was greatly extended. This dual spectral capability also made it possible to invoke various data integrity safeguards.

The REDAR IV system acquired, monitored, displayed, and recorded all survey data for each second of real time. The data stored on magnetic tape consisted of the dual spectral data, as mentioned previously, and environmental data such as outside air temperature and absolute barometric pressure. It also included positional data derived from a UHF radio ranging system (URS) and radar altimeter. The REDAR IV system then processed this positional data in real time to provide a navigational display for the helicopter pilot.

The survey was conducted in three segments. First, a background survey was performed that encompassed the entire KSC and CCAFS area. Then, two smaller, but highly detailed surveys were conducted: the first focused on Launch Complexes 39A and 39B, and the second on the Shuttle Landing Facility. Survey operations were based at the NASA hangar (No. 751) at Patrick Air Force Base, located about 12 miles south of CCAFS. Permanent electric power and telephone service were installed to support the mobile computer van for this and future surveys. All flight operations were conducted under day VFR conditions only. Each day's flights were scheduled 24 hours in advance with the Eastern Test Range Scheduling Office in close coordination with Patrick AFB Radar Approach Control.

Prior to commencement of survey flight operations, two flights were conducted during an equipment setup day to initialize and validate the aircraft positioning and the real-time navigation system.

The background survey was performed to provide an overview of the radiological character of the entire KSC and CCAFS area and to document the present radiological conditions. This survey segment was first conducted to become familiar with the area, the air traffic control procedures, and any navigational hazards. A series of 12 flights were conducted during a 10-day period to complete this segment. The area surveyed is that enclosed by the survey boundary as denoted in Figures 1 and 2. This boundary roughly corresponds to the boundaries of the KSC and CCAFS reservations, less large expanses of water. The area encompassed approximately 200 square miles (500 square kilometers). It was surveyed with a regular grid of 207 parallel flight lines ranging in length from 1 to 26 miles (1.6 to 41 kilometers). These lines were spaced 500 feet (152 meters) apart and flown at an altitude of 300 feet (91 meters) above ground level (AGL) and with an airspeed of 80 knots (147 kmph). The lines were oriented so that they paralleled the shoreline between the Atlantic Ocean and Mosquito Lagoon north of Launch Complexes 39A and 39B, that is, roughly parallel to the SLF. This orientation both minimized the number of short flight lines and maximized the length of the lines flown, thereby reducing the total flight time required for completion. Four areas were not surveyed within the survey boundary due to vertical obstructions or navigational hazards. These included the immediate area surrounding the launch pads at Complexes 39A and 39B, the Vehicle Assembly Building, and bunkers near Port Canaveral. The areas not surveyed are indicated in Figures 1, 2, and 3 by regions of blue cross-hatching.

The two detailed surveys were conducted using the same high sensitivity, high resolution methods that would be employed to search and map an area for the anomalous low energy gamma radiation

* Radiation and Environmental Data Acquisition and Recorder system, Model IV.

** Messerschmitt-Bolkow-Blohm (MBB) BO-105.


CONVERSION SCALE

| LETTER LABEL | TOTAL EXPOSURE RATE AT 1 m ALTITUDE ($\mu$R/h)* |
|---|---|
| A | < 3.7 |
| B | 3.7 - 4.0 |
| C | 4.0 - 5.0 |
| D | 5.0 - 6.5 |
| E | 6.5 - 9.0 |

* Contours indicate total gamma ray exposure rate extrapolated to 1 m above the ground due to terrestrial sources and cosmic rays, inferred from gamma count rates observed at 91 m altitude. Extrapolation valid only over large areas comparable to the detector's field-of-view. Cosmic rays contributed 3.6 $\mu$R/h to the reported values.

**FIGURE 1.** ***ISORADIATION CONTOURS OF TOTAL EXPOSURE RATE SUPERIMPOSED ON AN AERIAL PHOTOGRAPH MOSAIC OF THE KENNEDY SPACE CENTER AND CAPE CANAVERAL AIR FORCE STATION - NORTH***


**CONVERSION SCALE**

| LETTER LABEL | TOTAL EXPOSURE RATE AT 1 m ALTITUDE (μR/h)* |
|---|---|
| A | < 3.7 |
| B | 3.7 - 4.0 |
| C | 4.0 - 5.0 |
| D | 5.0 - 6.5 |
| E | 6.5 - 9.0 |
| F | 9.0 - 15 |
| G | 15 - 75 |
| H | 75 - 200 |
| I | 200 - 350 |

*Contours indicate total gamma ray exposure rate extrapolated to 1 m above the ground due to terrestrial sources and cosmic rays, inferred from gamma count rates observed at 91 m altitude. Extrapolation valid only over large areas comparable to the detector's field-of-view. Cosmic rays contributed 3.6 μR/h to the reported values.

**FIGURE 1.** ***ISORADIATION CONTOURS OF TOTAL EXPOSURE RATE SUPERIMPOSED ON AN AERIAL PHOTOGRAPH MOSAIC OF THE KENNEDY SPACE CENTER AND CAPE CANAVERAL AIR FORCE STATION - SOUTH (CONCLUDED)***


**FIGURE 2.** ***MAN-MADE GROSS COUNT ISOPLETHS SUPERIMPOSED ON AN AERIAL PHOTOGRAPH MOSAIC OF THE KENNEDY SPACE CENTER AND CAPE CANAVERAL AIR FORCE STATION - NORTH***


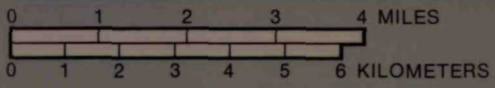




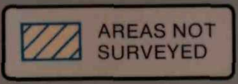


**CONVERSION SCALE**

| LETTER LABEL | RELATIVE ABUNDANCE* |
|---|---|
| A | < 3 |
| B | 3 - 5 |
| C | 5 - 10 |
| D | 10 - 30 |
| E | 30 - 100 |
| F | 100 - 300 |
| G | 300 - 1000 |
| H | 1000 - 1500 |

*Contours indicate anomalous, non-natural gamma radiation at energies of 40 to 1394 keV. The magnitude indicated is the radiation flux in excess of background levels and reported in multiples of the standard deviation in the MMGC.

**FIGURE 2.** ***MAN-MADE GROSS COUNT ISOPLETHS SUPERIMPOSED ON AN AERIAL PHOTOGRAPH MOSAIC OF THE KENNEDY SPACE CENTER AND CAPE CANAVERAL AIR FORCE STATION - SOUTH (CONCLUDED)***

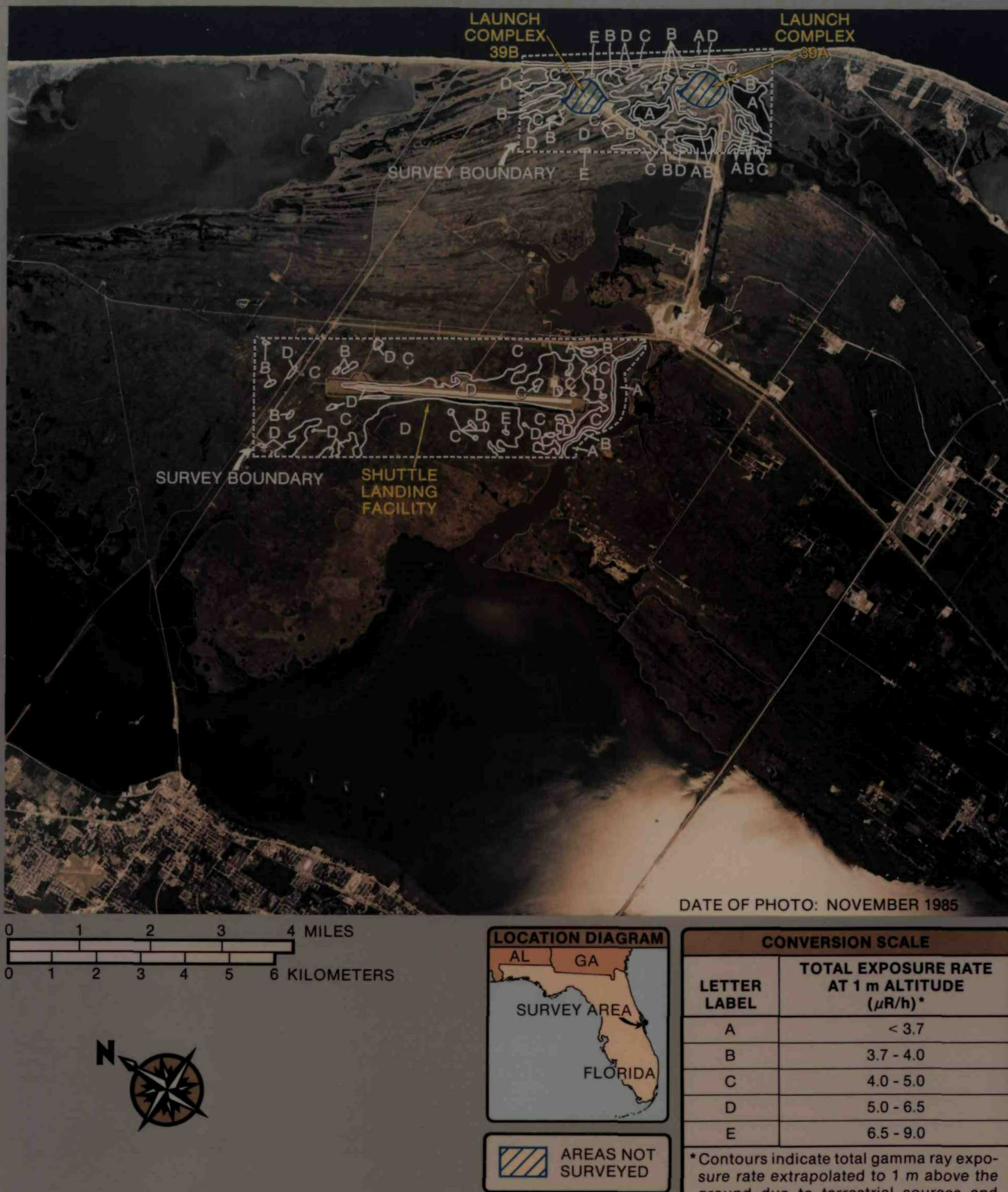


**CONVERSION SCALE**

| LETTER LABEL | TOTAL EXPOSURE RATE AT 1 m ALTITUDE ($\mu$R/h)* |
|---|---|
| A | < 3.7 |
| B | 3.7 - 4.0 |
| C | 4.0 - 5.0 |
| D | 5.0 - 6.5 |
| E | 6.5 - 9.0 |

*Contours indicate total gamma ray exposure rate extrapolated to 1 m above the ground due to terrestrial sources and cosmic rays, inferred from gamma count rates observed at 30 m altitude. Extrapolation valid only over large areas comparable to the detector's field-of-view. Cosmic rays contributed 3.6 $\mu$R/h to the reported values.

**FIGURE 3.** ***ISORADIATION CONTOURS OF TOTAL EXPOSURE RATE SUPERIMPOSED ON AN AERIAL PHOTOGRAPH OF THE SHUTTLE LANDING FACILITY AND LAUNCH COMPLEXES 39A AND 39B***

that would be characteristic of $^{238}Pu$. That is, these surveys were conducted at the lowest altitude, the slowest speed, and with the narrowest line spacing as was practical. The parallel lines were spaced 200 feet (61 meters) apart and flown at an altitude of only 100 feet (31 meters) AGL and airspeed of 60 knots (110 kmph). The lines flown in both of the detailed surveys were oriented the same as those flown in the background survey described previously.

The first of these detailed surveys was conducted over Launch Complexes 39A and 39B. It is believed that most of the radiological impact due to an accident on the launch pad would be confined to a radius of about 3,000 feet (915 meters). Therefore, a survey boundary was defined that included both launch sites plus a substantial margin, 1,200 feet (366 meters), beyond this 3,000-foot radius. The 5.5-square-mile (14-square-kilometer) area, denoted in Figure 3, was surveyed in a single flight. A grid of 42 parallel lines was required to cover this 1.6-mile wide by 3.4-mile long (2.5-kilometer by 5.5-kilometer) area. The aerial cables surrounding the launch pads prevented flying survey lines near the launch platforms. In fact, the unflyable area was larger for the lines flown at 100 feet AGL than those flown at 300 feet AGL because the highest point of suspension of the cables was on the launch platform at the center of the unflyable area.

The second detailed survey was conducted over the Shuttle Landing Facility. This 8.5-square-mile (22-square-kilometer) survey area, also denoted in Figure 3, extends 4,600 feet (1.4 kilometers) on either side of the runway. The survey boundary was defined to be 1 mile (1.6 kilometer) north of the runway threshold terminating just 0.5 mile (0.8 kilometer) south of the end of the runway over Banana Creek. This provides an ample margin around the runway. The 1.7-mile by 5-mile (2.7 kilometers by 7.9 kilometers) area was surveyed with 46 lines acquired on two flights in a single day.

In order to assure data integrity and facilitate analysis, diagnostics were performed routinely before each flight. Detector backgrounds due to aircraft, radon, and cosmic ray contributions were estimated from measurements made well off-shore over the ocean while enroute to and from the survey area. An expanded description of the equipment is presented in Appendix A.

## 4.2 Data Reduction Procedures

The data were processed to produce contour plots of total exposure rate, man-made gross count (MMGC), and $^{238}Pu$ concentration. Contour plots of total exposure rate were produced and are presented for all three surveys. A contour plot of man-made gross count was produced for all three surveys, but it is presented only for the background survey of KSC and CCAFS. The man-made gross count contour plots were omitted for Launch Complexes 39A and 39B and the SLF survey area because no man-made radioactivity was present. Hence, these contour plots are featureless. Likewise, although many $^{238}Pu$ extraction procedures were evaluated and contour plots produced for Launch Complexes 39A and 39B and the SLF survey area, no plutonium contour plots are reported for the same reason. However, the $^{238}Pu$ extraction procedures were used to estimate sensitivity limits for detection of both infinite planar surface distributions and point sources of $^{238}Pu$. These data reduction and analysis procedures are briefly described in this section. Additional discussions of the data processing procedures employed can be found in Appendix B.

The principal representation of the results from all three survey segments is an isoradiation contour map of total exposure rate due only to gamma ray emitters. The results are exhibited in Figures 1 and 3 and discussed in Section 5.0. The values reported represent averages over a large area. That is, two-thirds of the photons observed originate from a radius which surrounds the detector on the ground that is approximately the same as the detector's altitude above ground level. These exposure rates are expressed in $\mu R/h$ as would be observed 1 meter above ground level. The total exposure rate is computed as follows. The terrestrial gross count rate is constructed by subtracting estimates of the aircraft, radon, and cosmic background contributions measured over a large body of water from each second of gross count rate measured at the survey site. Corrections for deviation from the prescribed altitude and counting losses are applied. The observed gross count rates are then converted to exposure rate by application of a suitable factor determined at a calibration range near Lake Mead in Arizona. Then, an estimate of the cosmic ray background exposure rate reported for the area is added. Finally, these data are contoured and superimposed on the aerial photograph mosaic of the survey area. This procedure is sometimes referred to as a gross count contour plot.

An alternate analysis, the man-made gross count contour, applied to the present data attempts to extract and map only radiation due to man-made radioactive materials. This procedure results in an enhanced representation of the spatial distribution of all man-made radioactive material which is relatively free from distortions due to variations in the natural background. The results are reported as isopleth contours indicating anomalous, non-natural radiation at energies between 40 keV and 1394 keV. The magnitude indicated is the radiation in excess of background levels reported in multiples of the standard deviation in the MMGC observed in a background area. This technique was applied to all three sets of survey data, but is reported only for the background survey (Figure 2). A discussion of the results is presented in Section 5.0.

The MMGC extraction procedure requires an estimate of the natural background radiation contribution to be subtracted from a portion of the energy spectrum that spans the energies characteristic of the common, man-made gamma emitters for each second of data. This net quantity, termed the man-made gross count, is then contoured and superimposed on the aerial photograph to yield the man-made gross count contour plot presented in Figure 2. This type of extraction technique is called a "two window" stripping procedure. The background window is the region of the spectrum that is dominated by natural background radiation, 1394 keV to 3008 keV. The spectral region containing the man-made radiation is called the signal window, 40 keV to 1394 keV. A detailed description of this procedure is presented in Appendix B.

Finally, the data were used to evaluate the merit of several similar stripping procedures for $^{238}$Pu. Merit was determined in terms of the ability of the extraction to isolate $^{238}$Pu. A good extraction is both sensitive to the presence of $^{238}$Pu and insensitive to variations in the local background radiation. The sensitivity of the stripping procedure to $^{238}$Pu is determined by computing the minimum detectable activity (MDA) required to be present in order to be "detected" by the aerial survey system. Two very different MDAs were considered. One MDA was defined for a uniform distribution of plutonium on the surface of flat ground, i.e., infinite planar surface source distribution. Another MDA was defined to be valid for either a small piece of plutonium or a uniform surface distribution that is very small compared to the detector's field-of-view, i.e., point source distribution. The effect of self-attenuation in the fuel was considered for the point source MDA computations. Each MDA was defined to be three times the product of an appropriate concentration conversion coefficient and the standard deviation in the net $^{238}$Pu count rate. Computation of the conversion coefficients is well beyond the scope of this discussion. However, these methods are described in detail in several special EG&G/EM reports.[7,8] Sensitivity to background variations was studied in two ways. First, the net $^{238}$Pu count rate computed by each procedure was graphically compared over dry land, marsh, and water. If the procedure has little sensitivity to background variations, then the differences between the above quantities would be small. A more laborious method requires production of a contour plot of the net $^{238}$Pu count rate for each extraction procedure to be considered.

A comparison of the MDAs and a graphic comparison of the net $^{238}$Pu count rates were performed for each of 12 stripping procedures. These results are reported in Section 5.0. All 12 procedures were of the two-window type, similar to the MMGC mentioned earlier. The difference between these $^{238}$Pu stripping procedures and the MMGC stripping procedure is the definition of the energy windows. Each procedure focused on a different plutonium photopeak or choice of background window.

The nine photopeaks associated with $^{238}$Pu are reviewed in Table 1. Three photopeaks near 765 keV appear as a single photopeak in an NaI(Tl) spectrum. These are referred to as the 765-Complex. It is this complex that is most commonly associated with $^{238}$Pu. The windows used in each of the extraction procedures that were evaluated are summarized in Table 2. The windows are defined in terms of energy and the channel numbers in the REDAR IV spectra. The photopeak labeled "PU238GC" is actually a window that spans the three lowest energy photopeaks: 43.5, 99.9, and 152.8 keV. Hence, a center window energy is not applicable. All other photopeak windows were chosen with energy limits of about ±8% of the center energy. This will accommodate a photopeak with a resolution not exceeding 16% Full Width at Half Maximum (FWHM).

Contour plots were produced for the two detailed surveys using only three extraction procedures, numbers 1, 2, and 6 in Table 2. The contour plots were featureless and, therefore, are not presented.

| Table 1. Photopeaks of $^{238}$Pu | |
|---|---|
| **Photon Energy (keV)** | **Fraction Emitted in Alpha Decay** |
| 43.5 | 3.94 $10^{-4}$ |
| 99.9 | 7.45 $10^{-5}$ |
| 152.8 | 1.02 $10^{-5}$ |
| 201.0 | 4.3 $10^{-8}$ |
| 742.8 | 5.6 $10^{-8}$ |
| 766.4 | 2.4 $10^{-7}$ |
| 786.3 | 3.6 $10^{-8}$ |
| 851.7 | 1.7 $10^{-8}$ |
| 1001.1 | 1.3 $10^{-8}$ |
| 765-Complex[1] | 3.33 $10^{-7}$ |

[1] Complex of three photopeaks: 742.8 (17%), 766.4 (72%), 786.3 (11%) keV.

## 5.0 SURVEY RESULTS AND DISCUSSION

The results of the aerial radiological surveys of the Kennedy Space Center and Cape Canaveral Air Force Station are reported in the following discussions. Figures 1 and 2 present the results of the background survey as contour plots of total external exposure rate and man-made gross count, respectively. The results of the two detailed surveys are reported together as contour plots of total exposure rate in Figure 3. Finally, the extraction evaluations and plutonium sensitivities are presented in Tables 3 and 4 in Section 5.3. Conclusions regarding mapping $^{238}$Pu are also presented.

### 5.1 Background Survey Results

The contour plot of total external exposure rate due to gamma radiation measured in the background survey is presented in Figure 1. The figure has been divided into two separate plates, north and south, to facilitate reproduction. The plates are of the same scale. Coverage in each figure overlaps approximately one-half mile (0.8 kilometer). The blue cross-hatched regions indicate areas not surveyed due to navigational obstructions. Exposure rate is reported in units of $\mu$R/h extrapolated to 1 meter above ground level. The exposure rates observed are generally quite low and relatively uniform. Hence, the exposure rate contour intervals were chosen to be closely spaced and, in some cases, to reflect the effect of the topography.

The observed exposure rate generally ranged from 3.7 to 6.5 $\mu$R/h (B, C, and D levels). In wet areas, B levels were more typical. However, a collection of small, E-level (6.5 to 9 $\mu$R/h) regions

**Table 2. Window Definitions for $^{238}$Pu Extractions**

| Extraction Procedure Number | Photopeak keV | Photopeak Window | | | Background Window | |
|---|---|---|---|---|---|---|
| | | Channels | Limits keV | Center keV | Channels | Limits keV) |
| 1 | 43.5 | 10,12 | 36 - 48 | 42 | 14,16 | 52 - 64 |
| 2 | 99.9 | 23,27 | 88 - 108 | 98 | 29,224 | 112 - 3,008 |
| 3 | 99.9 | 23,27 | 88 - 108 | 98 | 29,33 | 112 - 132 |
| 4 | 152.8 | 36,42 | 140 - 168 | 154 | 44,224 | 172 - 3,008 |
| 5 | 152.8 | 36,42 | 140 - 168 | 154 | 44,50 | 172 - 200 |
| 6 | PU238GC | 10,42 | 36 - 168 | N/A | 45,224 | 176 - 3,008 |
| 7 | PU238GC | 10,42 | 36 - 168 | N/A | 44,99 | 172 - 584 |
| 8 | 201.0 | 46,54 | 180 - 216 | 198 | 56,224 | 220 - 3,008 |
| 9 | 765-Complex | 108,121 | 680 - 848 | 764 | 123,224 | 860 - 3,008 |
| 10 | 765-Complex | 108,121 | 680 - 848 | 764 | 123,136 | 860 - 1,028 |
| 11 | 851.7 | 116,127 | 776 - 920 | 848 | 128,224 | 930 - 3,008 |
| 12 | 1,001.1 | 128,141 | 920 - 1,088 | 1,004 | 142,224 | 1,100 - 3,008 |

were observed to form a north-south strip about 3 miles (5 kilometers) east of the KSC industrial area. The strip extends about 3 miles north of the survey boundary. Exposure rates were also elevated in the vicinity of all developed areas, such as the industrial areas, Vehicle Assembly Building, and launch pads. The highest exposure rate observed in these areas was in the 6.5 to 9 $\mu$R/h range (E level). Spectral analyses in these areas indicate that higher levels of $^{214}$Bi, characteristic of natural uranium, are the cause. This suggests that the enhanced radiation level is due to the import of building material, i.e., gravel or concrete, whose radioactive constituents are not characteristic of Merritt Island. Exposure rates at Launch Complexes 39A and 39B and, generally, at the Shuttle Landing Facility were in the 5 to 6.5 $\mu$R/h range (D level). A very prominent radiation anomaly with an apparent exposure rate up to level I (200 to 350 $\mu$R/h) was located about 1 mile (1.6 kilometers) east of the CCAFS industrial area. The actual exposure rate is expected to be about 1,000 times greater than indicated because of the large area averaging. The anomalous radiation was identified to be from a 19 curie $^{192}$Ir source being used at that time for industrial radiography in Building 1663. The compression of the contours on the southeast side of this anomaly indicates that the source was shielded or removed by the time the helicopter flew the next adjacent line to the southwest. Due to averaging over large areas by the aerial detection system, exposure rates reported over highly localized anomalies such as this may be underestimated by as much as a factor of 1,000. This effect, although to a less significant degree, leads to incorrect estimation of exposure rates over creeks, islands, and ponds. For example, the exposure rate over a small pond surrounded by land would be overestimated. Conversely, the exposure rate over a small island surrounded by water would be underestimated. Because of this effect, in marshy areas, where there are many small dry and wet areas within the detector's field-of-view, the reported exposure rates may be difficult to reconcile with ground-based measurements.

The results of the man-made gross count extraction are presented in Figure 2 which also has been divided into two plates (north and south). Strong suppression of variations in natural background radiation is evident and new features emerge. Values are reported in multiples of the typical standard deviation in the MMGC count rate. The northern plate exhibits almost entirely A level, indicating small variations in the MMGC of three standard deviations or less. Only three regions in the northernmost end of the survey area are B level, which indicates a modest deviation in the MMGC of three to five standard deviations. The southern plate exhibits a larger B-level area, especially in the north-south strip where the exposure rate was observed to be elevated, as mentioned earlier. Several C-level anomalies, indicating variations of 5 to 10 standard deviations, encircle the VAB, the small building one-half mile east of the VAB along the crawlerway, the vertical integration building, a portion of the CCAFS industrial area, and much of the KSC industrial area. The small building along the crawlerway has been identified as a non-destructive evaluation facility containing several radiographic sources. In fact, two D-level (10 to 30 standard deviations) anomalies are found in the KSC industrial area. The $^{192}$Ir anomaly is very strongly indicated with an H level (1,000 to 1,500 standard deviations).

Areas designated as "A" level should be interpreted as being free of sources of man-made radioactivity. Areas labeled as "B" level indicate a significant change in the radioactive constituency which is generally natural but may be due to the presence of a weak, man-made source of radioactivity. Level C and above can usually be assumed to represent the presence of man-made radioactivity. However, spectral analyses of all the anomalies seen in Figure 2 indicate only the presence of excess $^{214}$Bi, excluding the $^{192}$Ir source described above. No man-made radioactive sources were identified except for the $^{192}$Ir source. Occasionally, a heavily shielded, man-made source will be detected by the MMGC extraction, but it will not be possible to produce a recognizable spectrum of the source. Moreover, an excess of $^{214}$Bi may also be due to the presence of radium, perhaps as paint or a source. Hence, these MMGC anomalies can neither be conclusively identified as natural nor man-made. Their identification as natural is generally favored by the data.

### 5.2 Launch Complexes 39A and 39B and Shuttle Landing Facility Survey Results

The results of the two high resolution, high sensitivity surveys conducted over the Shuttle Landing Facility and over Launch Complexes 39A and 39B are presented in Figure 3. The results are reported as isoradiation contours of exposure rate superimposed on a portion of the aerial photograph mosaic used for previous figures. To facilitate comparison of these results to those of the background survey, the exposure rate contour intervals, as well as the scale and orientation of the figures, were defined to be the same. In general, the contours are much more complex in both of these survey areas than those seen in the background survey due to the increased resolution. The value of these two detailed surveys is not what they reveal about exposure rate here, but rather as a baseline for comparison in the event of a radiological accident.

The results of the detailed survey of Launch Complexes 39A and 39B are in good agreement with those of the background survey although they are markedly different in appearance. Throughout this area, C-level exposure rates (4.0 to 5.0 $\mu$R/h) prevailed, particularly in marshy areas. Drier areas such as the launch pads exhibited D-level exposure rates (5.0 to 6.5 $\mu$R/h). The highest exposure rates, E-levels (6.5 to 9.0 $\mu$R/h), were observed in three isolated areas around the perimeter of the launch pads. Notice that the area not surveyed in the immediate vicinity of the launch pads is somewhat larger in this detailed survey than was the case in the background survey. Finally, individual bodies of water caused localized depressions of the exposure rate to A and B levels (3.7 to 5.0 $\mu$R/h).

The results of the Shuttle Landing Facility detailed survey are also in agreement with the background survey. Generally, C-level exposure rates were observed in this area except to the southwest of the runway where there was a large D-level region (5.0 to 6.5 $\mu$R/h). The exposure rate along the entire runway was also D level. Scattered B-level regions and an isolated E-level region can be identified.

### 5.3 Sensitivity for $^{238}$Pu

The MDAs for an infinite planar surface source and a point source are reported in Tables 3 and 4, respectively. These results are computed rather than directly measured. The calculated MDA values utilized the extraction count rate uncertainties, i.e., standard deviations, that were observed in the survey data at the designated altitude. The count rate conversion coefficient calculation assumed a cosine-like detector angular response function.

**Table 3. Minimum Detectable Activities for an Infinite Planar Surface Distribution of $^{238}$Pu**

| Extraction Procedure Number | Photopeak (keV) | MDA at 100 Feet AGL (mCi/m$^2$) | MDA at 300 Feet AGL (mCi/m$^2$) |
|---|---|---|---|
| 1 | 43.5 | 1.5 | 11. |
| 2 | 99.9 | 0.72 | 4.6 |
| 3 | 99.9 | 0.87 | 2.9 |
| 4 | 152.8 | 3.3 | 11. |
| 5 | 152.8 | 3.9 | 10. |
| 6 | PU238GC | 2.4 | 14. |
| 7 | PU238GC | 2.4 | 11. |
| 8 | 201.0 | 660 | 2,000 |
| 9 | 765-Complex | 70. | 120 |
| 10 | 765-Complex | 85. | 130 |
| 11 | 851.7 | 860 | 1,800 |
| 12 | 1,001.1 | 960 | 2,800 |

| Table 4. Minimum Detectable Activities for a $^{238}$Pu Point Source | | | | | |
|---|---|---|---|---|---|
| Extraction Procedure Number | Photopeak (keV) | MDA at 100 Feet AGL (Ci) | | MDA at 300 Feet AGL (Ci) | |
| | | Self-Attenuated | Not Self-Attenuated | Self-Attenuated | Not Self-Attenuated |
| 1 | 43.5 | 24 | 1.1 | 4,000 | 35 |
| 2 | 99.9 | 11 | 4.5 | 1,200 | 130 |
| 4 | 152.8 | 170 | 25 | 9,000 | 390 |
| 8 | 201.0 | 180,000 | 5,700 | 12,000,000 | 97,000 |
| 9 | 765-Complex | 1,300 | 950 | 12,000 | 6,200 |
| 11 | 851.7 | 22,000 | 11,000 | 350,000 | 98,000 |
| 12 | 1,001.1 | 24,000 | 13,000 | 540,000 | 160,000 |

Consider first the MDAs calculated for an infinite planar surface source. These are summarized in Table 3. The calculation assumes that the source material is present only on the surface and that no shielding material overlays this source material. Infiltration of the source material into the soil or shielding due to vegetation or standing water will reduce the sensitivity of the aerial system, particularly for extractions employing low energy photopeaks. The uncertainty in the values reported may be as great as a factor of two.

The most sensitive extractions for a planar surface distribution of plutonium are those that make use of the three lowest energy photopeaks. This may seem surprising because $^{238}$Pu is usually most strongly characterized by the 765 keV photopeak complex, while these three photopeaks often appear to be quite weak. The reason the three lowest energy photopeaks sometimes appear weak, even though they are actually emitted 1,000 times more than the 765 keV complex, is that they are very strongly attenuated by the plutonium itself (self-attenuation) and by any container walls that may be present. Little self-attenuation occurs for a fine dispersion of plutonium scattered widely on the surface of the ground. Hence, these low photopeaks are easily observed and permit a sensitive extraction.

One would expect that the PU238GC strips which combine the sensitivity of all three photopeaks would have been the best to detect a planar plutonium source. However, the strip for the 99.9 keV photopeak was actually observed to be best at both altitudes. This is because there is so much more uncertainty, about 5 times, in the strip count rate for the broad energy window spanned in the PU238GC procedure than that for the narrow windows used to strip the individual photopeaks. Similarly, selection of broad background windows, e.g., extraction procedures 2, 4, and 6, would be expected to reduce the statistical uncertainty of the strip and result in improved sensitivity. But these broad windows introduce considerable sensitivity to background variations, particularly involving land versus water. Hence, the uncertainty is somewhat greater and the sensitivity correspondingly lower. However, if the uncertainty is based on data acquired just over land and systematic over-subtraction of background over water is acceptable, then the uncertainty is greatly reduced. Consequently, the strips using broad background windows become significantly more sensitive than their narrow window counterparts. Extraction procedures utilizing the other photopeaks, including the 765 keV complex, are not useful because they seriously lack sensitivity.

Consider next the MDAs computed for a point source (see Table 4). A point source is typically a single piece of source material. But a point source may also be a planar surface distribution that is much smaller in spatial extent than the detector's field-of-view. Therefore, two MDA values are reported for each altitude: one that includes the effect of self-attenuation and another that excludes this effect. If only a single point source is within the detector's field-of-view, the self-attenuated MDA is most appropriate. However, if the source material is finely divided but confined to a small area, then the MDA that excludes self-attenuation is more appropriate. The MDA for all real physical situations will lie between these limits. The effect of self-attenuation is computed by assuming that the source material is plutonium dioxide (80% $^{238}Pu$, 20% $^{239}Pu$), unshielded by cladding and spherical in shape. Departure from a spherical shape generally enhances detectability. The effect of fuel cladding on detectability is extremely severe for photons of less than 100 keV and nearly negligible above 800 keV. The effect of a substantial lateral displacement away from direct overflight of the source is included in the computation of the MDAs. That is, a lateral displacement of 140 feet (43 meters) was assumed for the 100-foot (31-meter) AGL survey where the line spacing was 200 feet (61 meters). For the 300-foot (91-meter) AGL survey which used a line spacing of 500 feet (152 meters), a lateral displacement of 300 feet was assumed. Direct overflight would generally reduce the MDAs by a factor of four or more. The calculation also assumes that the source is on the surface of the ground. Table 4 reports MDAs for only 7 of the 12 stripping procedures, one for each photopeak. That is, only the extractions with broad background windows were evaluated, and the PU238GC strips were eliminated. For reference purposes to the window definitions in Table 2, the extraction procedure numbers are preserved in Table 4. Comments regarding the broad background window extractions raised in the planar surface source discussion above also apply here. Uncertainties in these calculated MDAs are expected to be less than a factor of two. The effect of fuel cladding can lead to an increase of the MDA by many orders of magnitude.

To appreciate the activities reported in Table 4, it is useful to consider the size and mass of a plutonium dioxide sphere corresponding to an MDA of interest. These can be computed simply from the specific activity (12.1 Ci/g) and the density (11.5 g/cm$^3$). For example, a sphere whose activity corresponds to the best self-attenuated MDA for 100 feet AGL (11 Ci) weighs 0.9 grams and is 2.5 mm in diameter. This sensitivity is adequate to detect small pieces of a GPHS fuel clad which contains 1,830 curies of plutonium. It is also adequate to detect large pieces of a LWRHU.

Several conclusions can be drawn with respect to these results. First, because of the very unfavorable photon branching ratios (see Table 1), the sensitivity of the aerial survey system to $^{238}Pu$ is poor. Environmental Protection Agency standards for unrestricted land use require surface contamination levels to be several orders of magnitude less than the aerial system MDAs. However, the aerial system is adequate to map areas that would present a serious radiological hazard. As expected, only the method employed in the 100-foot AGL survey is really useful for mapping plutonium, particularly if point sources are present. The best extractions to map either a planar surface distribution or locate small point sources of plutonium are those for the lowest energy photopeaks, i.e., 1 and 2. If point sources are potentially large or may be clad, then the strip for the 765 keV complex (extraction procedure 9) is also quite useful.

# APPENDIX A
# SURVEY AND DATA ANALYSIS EQUIPMENT

## Survey Equipment

A Messerschmitt-Bolkow-Blohm (MBB) BO-105 helicopter (Figure A-1) is used as the aerial measuring platform. This aircraft, powered by two turbine engines, is safe, highly maneuverable, and well-suited for low altitude survey operations. Ordinary survey operations require a pilot and a technician to operate the sophisticated REDAR IV* data acquisition system.

FIGURE A-1. *MBB BO-105 HELICOPTER*

The detector array is carried in two external cargo pods mounted on the landing skids of the helicopter. This array consists of eight thallium-activated sodium iodide, NaI(Tℓ), "log" style scintillation detectors, each 4-in. square by 16-in. long (10.2 cm by 40.6 cm). Four of these detectors in each pod are positioned adjacent to one another to form a single 8-in. by 32-in. array. A lead and cadmium graded shield covers each array of four detectors so that only the 8-in. by 32-in. side facing the ground is exposed. The angular response of this array approximates a cosine function, particularly at low energies, i.e., less than 1 MeV. A small lead and cadmium collimated 4-in. diameter by 4-in. thick (10.2 cm by 10.2 cm) NaI(Tℓ) detector was also installed in one pod to measure radiation in very high gamma flux areas. The preamplifier outputs from the eight log detectors are carefully combined into one signal. The signal from the remaining small detector is processed by electronics identical to those used in the multiple detector sum. The eight log-detector and small single-detector signals are then each input to respective analog-to-digital converters (ADCs) in the REDAR IV dual multichannel analyzer (MCA) system. The gains and offsets for each of the nine detectors are adjusted so that photopeaks from the $^{22}Na$ and $^{241}Am$ calibration sources appear in preselected channels of both REDAR IV MCAs.

Division of the detectors into an eight log detector component and a single detector component results in each MCA exhibiting much different sensitivities. This greatly extends the effective count rate operating range of the REDAR IV system. That is, in areas where levels of radiation are so high that the eight detectors' signal suffers unacceptable counting losses and spectral distortions due to system dead time and pulse pileup, the single detector continues to provide valid data. An additional feature of the dual MCA acquisition technique is that it permits several data integrity safeguards to be invoked.

The REDAR IV is much more than dual MCA's. The REDAR IV, shown in Figure A-2, is a multi-microprocessor based real-time data acquisition, analysis, and recording system. The entire package design is compact and engineered for use in severe vibration and meteorological environments such as encountered in the aircraft or vehicles used in field surveys. The keyboard interactive control system displays all radiation data and system parameters to the operator via CRT monitors and various numeric displays.

Positional data and navigational parameters are also acquired, processed, and displayed to the operator with a separate special navigational display for the pilot. All radiation, positional, and certain environmental data are digitally recorded by the REDAR IV on magnetic tape cartridges for post-mission analysis.

The REDAR IV system, which employs a combination of five Z-80* microprocessors and two

---

* Radiation and Environmental Data Acquisition and Recorder system, Model IV.

* Zilog, Inc., Cupertino, California.

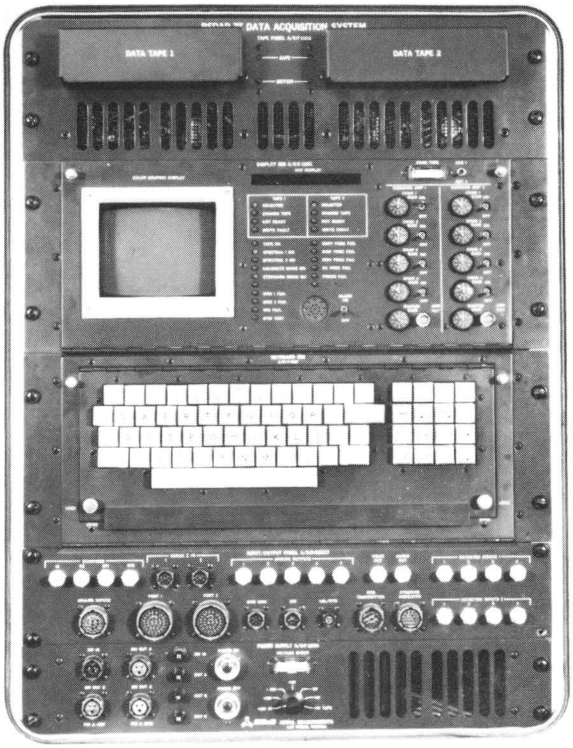

**FIGURE A-2.** ***REDAR IV DATA ACQUISITION SYSTEM***

AM9511* floating point arithmetic processors, is composed of the following six subsystems:

1. Radiation data acquisition system
   a. Dual MCA's
   b. Four Scalers
2. General data acquisition system which includes five analog channels
3. Real-time data analysis system using interactive keyboard
4. CRT display system
5. Positional data and navigation system
   a. UHF or microwave ranging system
   b. Radar altimeter
   c. Steering processor
   d. Pilot's navigational display
6. Magnetic tape recording system
   a. Dual tape drives digitally record all survey data acquired and system parameters

A block diagram of the REDAR IV system is presented in Figure A-3.

Each MCA collects a 1024-channel gamma ray spectrum, scaled to 4 keV per channel, once every second during the survey operation. The 1024-channel spectrum is compressed into 256 channels before storage on magnetic tape, remapping it according to the partitions summarized in Table A-1.

Compression of the spectrum in this manner does not result in significant loss of spectral resolution since the resolution of NaI(Tℓ) scintillators scales approximately linearly with energy. That is, the width of photopeaks, in channels, are nearly the same in all three partitions; therefore, photopeak identification and stripping techniques are not compromised. Yet, this compression reduces the data storage requirement by a factor of four.

Each of the 256-channel spectra is collected for one second then buffered by the spectral memory. The memory consists of two blocks of four buffers for each of the 256-channel spectra. One block accumulates four 1-second pairs of spectra while the other block is recorded on magnetic tape. The blocks then alternate between data accumulation and tape storage functions.

All data acquired by the REDAR IV system are buffered and recorded on magnetic tape as described above. Other radiation data acquired include live and real data accumulation times for each spectrum. These are employed in subsequent data processing to monitor and correct for counting losses due to system dead time. Environmental data, such as absolute barometric pressure and outside air temperature, are similarly recorded.

The REDAR IV system also acquires helicopter positional data which is then processed to provide a navigational display for the pilot. Geographic position is determined from a UHF or microwave ranging system (URS or MRS*) consisting of a master transponder with two slaves and navigational processors in the REDAR IV. The master transponder, mounted in the helicopter, interrogates two slave transponders, mounted on tall structures or high terrain, outside the survey area. By measuring the round-trip propagation time between master and slave stations, the distance to each can be computed. These distances are measured each quarter-second, but recorded only once each second.

---

*Advanced Micro Devices, Sunnyvale, California.

*URS: Trisponder/545. MRS: Trisponder/202A, Del Norte Technology, Inc., Euless, Texas.

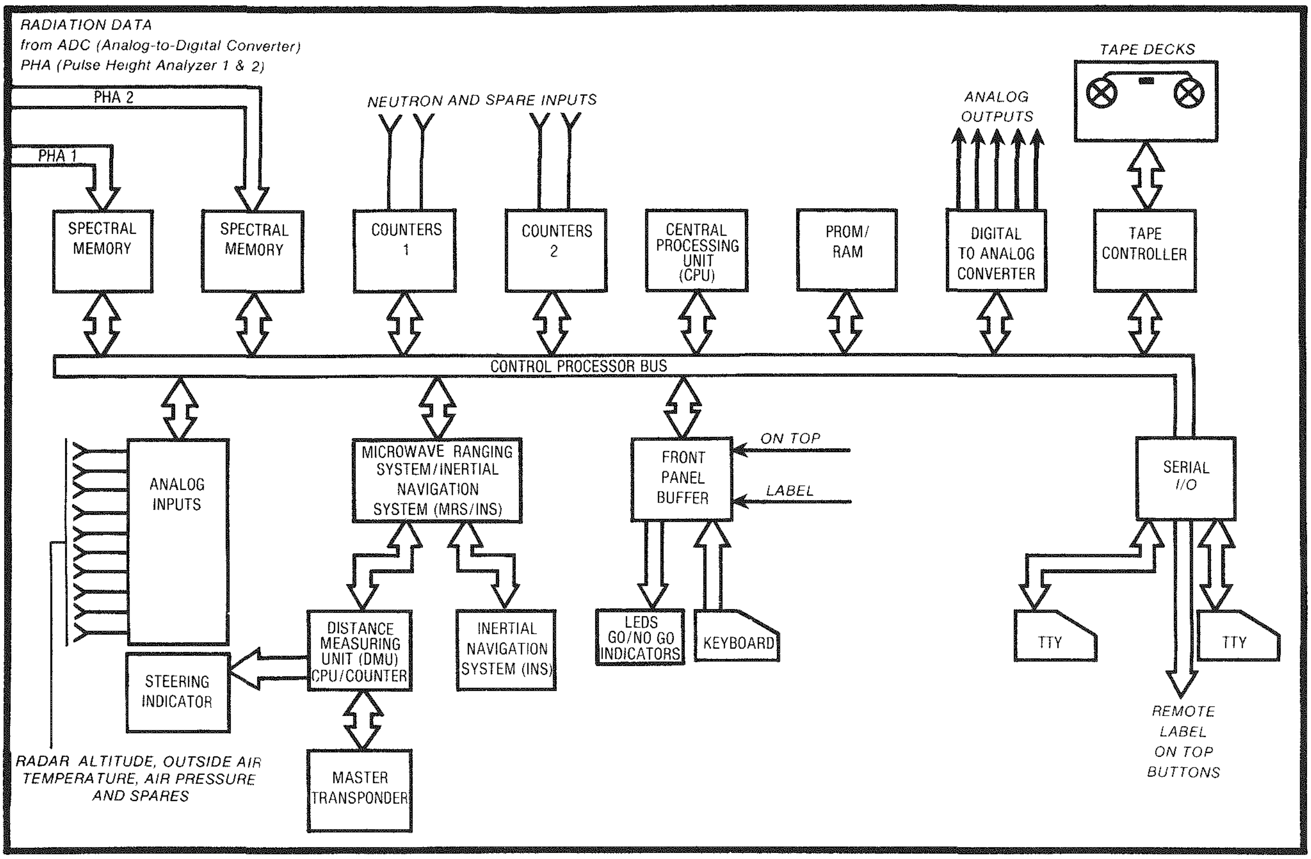


**FIGURE A-3.** ***REDAR IV PROCESSOR SYSTEM BLOCK DIAGRAM***

In order to survey an area fully and uniformly, a series of parallel survey lines are flown as generated by the REDAR IV steering processor and predefined by the operator. The steering processor utilizes the quarter-second positional data to compute present course error which is displayed to the pilot.

The helicopter's altitude above ground level is determined with a radar altimeter which measures the time delay of a microwave pulse echo and converts this to aircraft altitude. These data are recorded on magnetic tape so that variations of the observed gamma count rate caused by altitude deviations can be corrected in subsequent data processing. The steering processor compares the radar altitude to the survey altitude specified by the operator in order to present a course-error display to the pilot.

**Table A-1. REDAR IV Spectral Data Compression Scheme**

| $E_\gamma$ (keV) | Channel Input | Energy Coefficient $\Delta E$ (keV/channel) | Compressed Channel Output |
|---|---|---|---|
| 0 - 300 | 0 - 75 | 4 | 0 - 75 |
| 304 - 1,620 | 76 - 405 | 12 | 76 - 185 |
| 1,624 - 4,068 | 406 - 1,017 | 36 | 186 - 253 |
| 4,072 - Cutoff | 1,018 - 1,022 | N/A | 254 |
| > Cutoff | Forced to Zero | N/A | 255 |

An optional inertial navigation system (INS) or LORAN system can also be employed in the REDAR IV navigation system. The INS is used to augment the MRS in situations where MRS navigation is compromised or impossible due to terrain relief or obstructions. LORAN is used only if remotely stationed transponders are not available and precision positioning is not required. Latitude and longitude coordinates output by the INS and LORAN are processed and stored on magnetic tape just as all other data acquired by REDAR IV. At present, the pilot's real-time navigational display is not driven by the INS or LORAN output.

### Data Analysis Equipment

A preliminary analysis of survey data can be performed in the field on a mobile computer analysis system immediately after each flight. The mobile system is installed in a 36-foot motor home which also serves as the field operations base. Ordinarily, this "data-van" is located near the survey site at the helicopter staging area.

The mobile computer system, REDAC*, consists of a Data General ECLIPSE S280 computer, a 554-megabyte hard disk, two dual density nine-track tape drives, two digital cartridge drives, a 34-inch high speed plotter, three user terminals (with printers), and a line printer. The system's program library includes all routines found to be useful for data processing. Generally, only an initial analysis is performed on the mobile computer system. A complete analysis is performed in the EG&G/EM laboratory in Las Vegas, Nevada using a larger and faster Data General MV-8000 System.

---

*Radiation and Environmental Data Analysis and Computer system

## APPENDIX B

## DATA PROCESSING METHODS

### Products of Data Processing

The principal objectives of an aerial radiological survey are to map the spatial distribution and abundance of gamma-emitting nuclides visible at the surface and to identify the isotopes responsible for these emissions. Generally, only two products of radiation data processing are required to realize the objectives. The most useful product is an isoradiation contour map superimposed on an aerial photograph or topological map. These contours are used to image the spatial distribution and intensity of the radiation contributed by all radionuclides present or, as in many cases, just a single isotope. Routinely produced contours include:

1. Gross Count - Images radiation due to all sources.
2. Man-Made Gross Count - Images only radiation due to man-made sources.
3. Isotopic Extraction - Images only radiation due to a particular radionuclide (e.g., $^{226}Ra$, $^{232}Th$, $^{241}Am$, $^{238}Pu$, or $^{60}Co$).

Gross count and isotopic extractions can be performed by manipulating windows defined in the gamma energy spectrum. These windows can be weighted, summed, subtracted, or ratioed to extract the photopeak count rates for any particular radionuclide or desired combination of radionuclides. Since these procedures can be performed as a function of position in the survey area, these count rates can be contoured and scaled to a map or photo. The contours of constant count rates (isopleths) represent constant radiation intensity; hence, the more intuitive term "isoradiation contour" is often preferred. The quantities contoured can be reported as simply count rate, exposure rate, or even as isotope concentration in the soil. Isoradiation contours representing contributions from all sources, i.e., gross count contour, are reported as exposure rates in $\mu$R/h extrapolated to 1 m above the ground. Generally, isoradiation contours for isotope extractions are reported only in terms of observed count rate, but they can be reported as soil concentration, if desired. However, the computation of an accurate soil concentration is difficult in many cases due to the uncertain depth profile of soil concentration and highly variable shielding, i.e., soil moisture, paving, buildings, etc. Specific radionuclides that are responsible for anomalies or contamination can be identified by production of gamma energy spectra which represent any desired portion of the survey area. Such spectra can be energy calibrated and stripped of background or undesired adjoining peaks. A typical energy spectrum of natural background radiation observed at survey altitude is presented in Figure B-1.

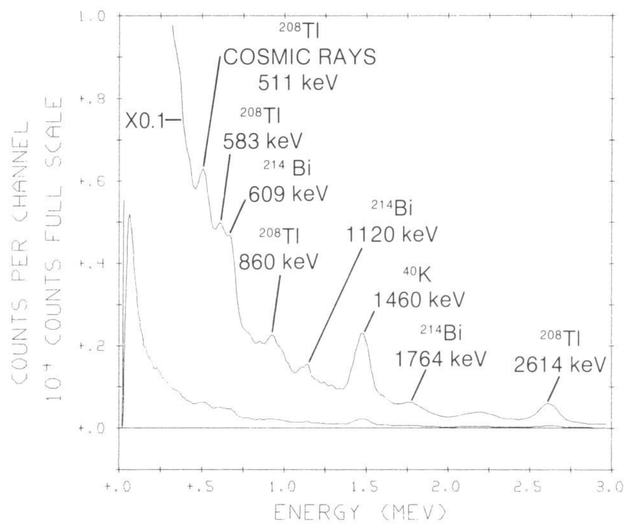


**FIGURE B-1.** ***GAMMA RAY ENERGY SPECTRUM TYPICAL OF THE BACKGROUND RADIATION OBSERVED OVER KSC AND CCAFS***

### Gross Count and Isotopic Extraction Procedures

The various extraction procedures share many features. For instance, the algorithm designed to generate and manipulate windows is the same in all cases. The primary differences appear in window selection and in the determination of weighting coefficients. Several particular extractions which exemplify the basic procedure and highlight necessary variations are presented below.

The gross count extraction is obtained from a single window defined to include all photopeaks in the entire energy spectrum due to terrestrial sources. A window W is defined as the sum of all counts observed between a maximum and minimum energy. The gross count can then be expressed as:

$$GC = [(A_e \bullet W_{gc}) \bullet Lt - C] \bullet Alt$$

where

$W_{gc}$ is the sum from $E_{min} = 0.04$ MeV to $E_{max} = 3.0$ MeV.

$A_e$ is the weighting factor (e.g., detector effective area normalization).

Lt is a live time counting loss correction.

C is background count rate.

Alt is a correction for altitude variations.

The background contribution C must be subtracted from the total window count rate to eliminate contributions due to: (1) sources of radiation within the helicopter and detector, (2) airborne radon and daughters, and (3) cosmic rays. This background is determined most simply by measuring the gross count (GC) over a large body of water, assuming no background. Since no terrestrial sources can be detected over a large body of water, the observed gross count is itself the combined background. Less accurate, alternative techniques of background determination can be used if no body of water is located near the survey site. Details of these methods exceed the scope of the present discussion.

Another single window extraction is used to isolate contributions due to $^{232}Th$. The window is then defined as the sum of the counts in the energy range 2.342 to 2.882 MeV, a $^{208}T\ell$ photopeak. The background is determined in the same manner in the gross count extraction.

A slightly more complex example is that of man-made gross count (MMGC) which employs two windows. This procedure is designed to extract a count rate related only to the presence of man-made radionuclides. Hence, the method must somehow eliminate contributions due to naturally-occurring radionuclides. Most common man-made isotopes exhibit photopeaks with energies between 0.04 and 1.39 MeV. Photopeaks observed above 1.40 MeV primarily arise from the dominant sources of natural radiation: $^{40}K$, $^{214}Bi$, and $^{208}T\ell$. Therefore, a window $W_{mm}$ (spanning the energy range 0.04 to 1.39 MeV) contains primarily natural and man-made source contributions, while window $W_n$ (from 1.40 to 3.00 MeV) usually contains only natural-source contributions. The man-made gross count can then be expressed as:

$$MMGC = A_e \bullet (W_{mm} - A_r W_n) \bullet Lt \bullet Alt$$

where the weight, $A_r$, is the ratio of counts due to natural sources in the two windows. That is, in an area where no man-made contamination is present,

$$A_r = \frac{W_{mm}}{W_n} \quad \text{Background only}$$

Thus, $A_r W_n$ is the number of counts expected in the man-made window due to natural sources. Hence, the difference, $W_{mm} - A_r W_n$, reflects counts generated only by man-made sources.

The $^{226}Ra$ extraction is also achieved with a two-window technique which differs from the man-made gross count extraction only in window location: the $^{226}Ra$ window, $W_{ra}$, sums counts from 1.576 MeV to 1.946 MeV. This collects counts from the photopeak of the decay daughter, $^{214}Bi$, which is higher in energy than any other natural source of radiation except for the $^{208}T\ell$ photopeak at 2.614 MeV.

The background window is defined to include the dominant $^{208}T\ell$ photopeak by letting $W_{T\ell}$ sum from 2.342 to 2.882 MeV. Hence, the extracted $^{226}Ra$ count rate can be expressed as:

$$RA = A_e \bullet (W_{ra} - A_r W_{T\ell}) \bullet Lt \bullet Alt$$

where $A_r$ is defined in a manner similar to that employed in the man-made gross count procedure.

An exhaustive description of all extraction is not practical in an appendix. It is sufficient to say that the above methods can be applied to most simple situations. Occasionally, more complex mixtures of radionuclides may be present and require more windows to be employed, but extension of the above techniques is straightforward.

# APPENDIX C
# SURVEY PARAMETERS

| | | | |
|---|---|---|---|
| Location | Kennedy Space Center and Cape Canaveral Air Force Station, Merritt Island and Cape Canaveral, Florida | | |
| Staging Area | Patrick Air Force Base, Florida, Hangar 751 | | |
| Survey Date | 9 through 23 October 1985 | | |
| Project Scientist | H W Clark | | |
| Survey Areas | Background | Complexes 39A and 39B | SLF |
| Survey Coverage | 200 sq mi | 5 5 sq mi | 8 5 sq mi |
| Survey Altitude | 300 ft | 100 ft | 100 ft |
| Line Spacing | 500 ft | 200 ft | 200 ft |
| Lines Surveyed | 207 | 42 | 46 |
| Speed | 80 knots | 60 knots | 60 knots |
| Detector Array | Eight 4-in square by 16-in long NaI(Tl) detectors and one 4-in diameter by 4-in thick NaI(Tl) detector, lead and cadmium shields installed | | |
| Acquisition System | REDAR IV using UHF Ranging System | | |
| Aircraft | MBB BO-105 Helicopter | | |

Data Processing

A Gross Counts
Window 0 04 - 3 0 MeV
Conversion Factor 910 cps per $\mu$R/h
Cosmic Ray Contribution 3 7 $\mu$R/h

B MMGC
Windows Signal 0 040 to 1 394 MeV, background 1 394 to 3 000 MeV
Typical background standard deviation 120 cps

C $^{238}$Pu extractions as specified in text

# REFERENCES


1 Jobst, J E 1979 "The Aerial Measuring Systems Program" *Nuclear Safety*, March/April 1979, 20 136-47

2 Bennett, G L , Lombardo, J J , and Rock, B J 1981 "Development and Use of Nuclear Power Sources for Space Applications" *Journal of the Astronautical Sciences* Oct -Dec , 1981, Vol XXIX, pp 321-342

3 Lindeken, C L , Peterson, K R , Jones, D E , and McMillen, R E August 1972 "Geographical Variations in Environmental Radiation Background in the United States" *Proceedings of the Second International Symposium on the Natural Radiation Environment, 7-11 August 1972, Houston, Texas* pp 317-332 Springfield, VA National Technical Information Service, U S Department of Commerce

4 Liboff, A R 1972 "Cosmic Ray Ionization in the Lower Atmosphere" *Proceedings of the Second International Symposium on the Natural Radiation Environment, 7-11 August 1972, Houston, Texas* pp 55-67 Springfield, VA National Technical Information Service, U S Department of Commerce

5 Boyns, P K 1981 *An Aerial Radiological Survey of Sandia National Laboratory and Inhalation Toxicology Research Institute* Report No EGG-1183-1779 Las Vegas, NV EG&G/EM

6 Boyns, P K 1976 *The Aerial Radiological Measuring System (ARMS) Systems, Procedures and Sensitivity* Report No EGG-1183-1691 Las Vegas, NV EG&G/EM

7 Stuart, T P 1976 *An HP 65 Computer Program for Calculating Discrete Source Detectability* Report No EGG-1183-1687 Las Vegas, NV EG&G/EM

8 Stuart, T P 1977 *Limiting Values for Radionuclide Concentrations in the Soil from Remote Spectrometer Measurements* Report No EGG-1183-1716 Las Vegas, NV EG&G/EM